
Speeding up Policy Simulation in Supply Chain RL

Vivek Farias
Sloan School of Management
Massachusetts Institute of Technology
Cambridge, MA 02139
vivekf@mit.edu

Joren Gijsbrechts
Esade Business School
Ramon Llull University
Barcelona, Spain
joren.gijsbrechts@esade.edu

Aryan Khojandi
Operations Research Center
Massachusetts Institute of Technology
Cambridge, MA 02139
khojandi@mit.edu

Tianyi Peng
Department of Aeronautics and Astronautics
Massachusetts Institute of Technology
Cambridge, MA 02139
tianyi@mit.edu

Andrew Zheng
Operations Research Center
Massachusetts Institute of Technology
Cambridge, MA 02139
atz@mit.edu

Abstract

Simulating a single trajectory of a dynamical system under some state-dependent policy is a core bottleneck in policy optimization algorithms. The many inherently serial policy evaluations that must be performed in a single simulation constitute the bulk of this bottleneck. To wit, in applying policy optimization to supply chain optimization (SCO) problems, simulating a single month of a supply chain can take several hours. We present an iterative algorithm for policy simulation, which we dub Picard Iteration. This scheme carefully assigns policy evaluation tasks to independent processes. Within an iteration a single process evaluates the policy only on its assigned tasks while assuming a certain ‘cached’ evaluation for other tasks; the cache is updated at the end of the iteration. Implemented on GPUs, this scheme admits batched evaluation of the policy on a single trajectory. We prove that the structure afforded by many SCO problems allows convergence in a small number of iterations *independent* of the horizon. We demonstrate practical speedups of 400x on large-scale SCO problems even with a single GPU, and also demonstrate practical efficacy in other RL environments.

1. Introduction

The core problems in supply chain optimization (SCO) all relate to managing inventory over time across some potentially large network of nodes, so as to match costly supply with uncertain demand. These problems are naturally viewed as dynamic optimization problems, albeit with intractable state-spaces that must track inventory and other resource levels across a large number of products and nodes. The development of detailed simulators (‘digital twins’) of supply chains in recent years has made SCO problems a ripe target for reinforcement learning.

A time-step in an SCO problem typically corresponds to either a demand or supply event; there are hundreds of millions of such events in a month for a large supply chain¹. As such, the task of simulating a fixed control policy is onerous, requiring the serial evaluation of the policy over a horizon, T , of tens or hundreds of millions of time-steps. For a policy parameterized by a non-trivial deep neural network (DNN), the task of simply simulating a *single sample path* under the policy can thus take several hours (or more) in the context of an SCO problem. This is an impediment to the application of RL to SCO problems; for instance, a policy optimization algorithm would require weeks of computation time even assuming a relatively small number of policy update iterations.

The key challenge above is the inherently serial nature of the task of simulation: the key computationally expensive step of evaluating a policy at a system state cannot be batched since the states encountered on a sample path are themselves computed serially. On the other hand, if an oracle were to reveal the sequence of T states encountered on the sample path being simulated, this computationally expensive task could be batched, and could even leverage the ‘single program multiple data’ paradigm GPUs are optimized for. Our goal here is to come close to this ideal via an iterative scheme.

1.1. This paper: the Picard Iteration

This paper proposes an iterative approach to policy simulation we dub the Picard iteration. Succinctly, while the Picard iteration applies to general policy simulation tasks, it provably yields a speedup in the context of SCO problems; in practice we show this speedup is greater than 400x.

The Picard iteration proceeds by dividing up the simulation horizon of T time-steps across (potentially, virtual) processes; the assignment of time-steps to processes may be informed by problem structure. We also initialize a ‘cache’ of actions, one for each time-step, that can be thought of as an initial guess of the actions that will eventually be simulated. Each process runs an independent simulation of the policy with an important tweak: a process only evaluates the policy on time-steps it has been assigned; on all other time-steps it simply uses the action for that time-step from the cache. As such, each process only takes time that is roughly proportional to the number of time-steps it is assigned. All processes run in parallel, with each process updating the cache in the time-steps it was responsible for. As such, a single Picard iteration is faster than the serial policy simulation task by a factor of roughly $\#\text{processes}$. How many such iterations are required to converge to the same outcome as serial policy simulation?

Provable speedup: We prove that in the context of a large class of SCO problems, the number of Picard iterations required to compute the same outcome as serial policy simulation is no more than the number of nodes in the supply chain. Thus, applied to such problems the Picard iteration yields an effective speedup of $\sim \#\text{processes}/\#\text{nodes}$. Since $\#\text{nodes}$ is at most a few hundred², and $\#\text{processes}$ can be scaled to tens of thousands via a GPU implementation, the Picard iteration guarantees a large speedup in policy simulation on SCO problems.

Practical speedup for SCO: We show that even on a single A100 GPU, the use of the Picard iteration yields an effective speedup of greater than 400x on policy evaluation for a large-scale SCO problem. The speedup displays attractive linear scaling with the number of processes (as predicted by our theory) and is *robust* across a range of challenging SCO problem instances. In addition, this speedup is persistent when scaling to an end-to-end RL pipeline.

Practical speedup for other problems: It is easy to show that in general problems we converge to the sequential simulation output after no more than T Picard iterations. Given its correctness in general, we explore whether the number of Picard iterations required is a lot smaller than T for problems outside SCO. Here we show that for a majority of OpenAI Gym MuJoCo environments, the Picard iteration could potentially yield a speedup of up to 40x.

1.2. Related literature

Supply Chain Optimization (SCO) problems represent a classic family of dynamic optimization problems with intractable state-spaces, and are becoming increasingly important due to the growing volumes in e-commerce. For instance, a 1% cost reduction in fulfillment for Amazon can be translated to about 1B US dollars savings [3]. Applying Deep Reinforcement Learning (RL) to solve intractable

¹<https://capitaloneshopping.com/research/amazon-orders-per-day/>

²Amazon has ~ 200 nodes [1]; Walmart has ~ 30 nodes in the U.S [2].

SCO problems has garnered increasing interest in recent years [4, 5, 6, 7]. Large companies such as Amazon [8], Alibaba [9], and JD.com [10] have reportedly been testing RL at scale in SCO contexts. Our motivation for this work is to eliminate the high costs of training and back-testing in these problems due to long horizons, T . While our framework is general, we showcase it on a representative problem in SCO: online fulfillment optimization [11, 12, 13, 14, 15, 16, 17, 18, 19].

There is a substantial body of literature on parallel reinforcement learning (see e.g., Asynchronous RL [20], RLlib [21], Envpool [22], and others [23, 24, 25, 26]), where embarrassing parallelism is implemented across different agents or rollouts. In contrast, Picard iteration specifically accelerates the evaluation of a single trajectory, which is particularly beneficial for real-world RL settings that often require training and back-testing on extensive historical data, thus *complementing* existing parallel RL techniques.

Methodologically, Picard iteration most closely resembles the optimistic branch of parallel computing for discrete event simulations [27]. Its workhorse approach is Time Warp [28, 29, 30], which has been recently extended to GPU [31]. In Time Warp, threads communicate via messages to determine if a rollback is needed, and if so, all newly generated events are removed. We implement a variant of Time Warp suitable to GPUs and show that while it yields some speedup, Picard iteration is almost two orders of magnitude faster; we attribute this to the inability to re-use policy evaluations computed on incorrect states within Time Warp.

Picard iteration leverages the batch computation power of GPUs to simulate sequential problems. Non-RL examples in this spirit include using lookahead decoding to increase the inference speed of LLM models [32] and a three-stage algorithm for simulating cellular base stations [33]. A distinctive feature of our approach is the theoretical guarantee of speedup, which captures the weakly-coupled structure of SCO problems. This is rare in the parallel computing literature. Moreover, the bound on the required number of Picard iterations may have broader implications for parallel computing, potentially serving as a complexity parameter for characterizing the coupling degree of a problem.

2. Model and algorithm

We consider a dynamical system with general state-space \mathcal{S} , action space \mathcal{A} , and a disturbance space Ω . The dynamical system itself is specified by a function $f : \mathcal{S} \times \mathcal{A} \times \Omega \rightarrow \mathcal{S}$. We assume the existence of an ‘always feasible’ action a^ϕ , so that for all s , $a^\phi \in \mathcal{A}(s)$, the set of feasible actions at state s . For our purposes a policy is simply a map $\pi : \mathcal{S} \times \Omega \rightarrow \mathcal{A}$; one may think of $\pi(\cdot)$ as a DNN and assume $\pi(s) \in \mathcal{A}(s) \forall s$. We may think of the disturbance here as capturing both exogenous shocks (e.g., demand in an SCO problem), as well as any randomization endogenous to π .

We next formally define the task of policy simulation. As input, we are given an initial state $s_1 \in \mathcal{S}$, a horizon T , and a sequence of disturbances $\{\omega_t : t \in [T]\}$. Our desired output is the sample path of actions under π , $\{a_t^{\text{seq}} : t \in [T]\}$ defined according to $a_t^{\text{seq}} = \pi(s_t, \omega_t)$, where $s_{t+1} = f(s_t, a_t^{\text{seq}}, \omega_t)$. We remark that we view the application of $\pi(\cdot)$, i.e. the computation $\pi(s, \omega)$ as computationally costly, while we view the application of $f(\cdot)$ given an action, $f(s, a, \omega)$ as computationally cheap. This is certainly the case in RL for SCO problems. Assuming a single application of $\pi(\cdot)$ takes unit time, our desire is to compute $\{a_t^{\text{seq}}\}$ in time $\ll T$.

We next present the Picard iteration. We assume M virtual processes indexed by m . Each m is assigned a disjoint partition of time-steps, $\mathcal{T}_m \subset [T]$ where $\cup_m \mathcal{T}_m = [T]$.

Algorithm 1 implicitly assumes the ‘cache’ of actions, $\{\alpha_t^k\}$ and the disturbance sequence $\{\omega_t\}$ sit in shared memory. Several remarks are in order:

Correctness: It is easy to see that the Picard iteration outputs the correct sequence of actions, i.e. $\{a_t^{\text{seq}}\}$ in at most T iterations. Observe that for the processor responsible for time-step $t = 1$, say m , $a_1^{1,m} = a_1^{\text{seq}}$. Consequently, $\alpha_1^1 = a_1^{\text{seq}}$. Thus, at iteration $k = 2$, the processor responsible for $t = 2$, say \tilde{m} , will take the correct sequential action at $t = 1$ and thus the correct sequential action at $t = 2$, i.e. $a_2^{2,\tilde{m}} = a_2^{\text{seq}}$, so that $\alpha_2^2 = a_2^{\text{seq}}$. Continuing in this fashion, we can show:

Proposition 1 *The Picard iteration converges in at most T iterations and returns $\{a_t^{\text{seq}}\}$.*

Algorithm 1 The Picard Iteration

```
1:  $k \leftarrow 1, \alpha_t^0 \leftarrow a^\phi$  for  $t \in [T]$  ▷ Initialize cache to always feasible action  $a^\phi$ 
2: while true do
3:   parfor  $m \leftarrow 1$  to  $M$  do ▷ Evaluate each process in parallel
4:      $s_1^{k,m} \leftarrow s_1$ 
5:     for  $t \leftarrow 1$  to  $T$  do
6:       if  $t \in \mathcal{T}_m$  then  $a_t^{k,m} = \pi(s_t^{k,m}, \omega_t)$  ▷ Process  $m$  evaluates  $\pi(\cdot)$ 
7:       else  $a_t^{k,m} = \alpha_t^{k-1}$  if  $\alpha_t^{k-1} \in \mathcal{A}(s_t^{k,m})$  (or  $a^\phi$  o.w.) ▷ Process  $m$  uses cached action
8:        $s_{t+1}^{k,m} = f(s_t^{k,m}, a_t^{k,m}, \omega_t)$  ▷ Process  $m$  updates its state
9:     end parfor
10:     $\alpha_t^k = a_t^{k,m}$  for  $m \leftarrow 1$  to  $M, t \in \mathcal{T}_m$  ▷ Process  $m$  updates cache on  $t \in \mathcal{T}_m$ 
11:    if  $\alpha_t^k = \alpha_t^{k-1} \forall t$  then return  $\{\alpha_t^k\}$  ▷ Converged
12:    else  $k \leftarrow k + 1$ 
```

While this proposition shows the correctness of the algorithm, it is not useful: if we required T iterations for convergence, we would achieve no speedup. We will later prove that Algorithm 1 converges in a small number of iterations *independent of T* in a large class of SCO problems.

Speedup and batching: A single iteration of Algorithm 1 achieves substantial speedup over sequentially computing $\{a_t^{\text{seq}}\}$. Specifically, assume that time-steps are divided up equally across all processes so that $|\mathcal{T}_m| \sim T/M$ for all m . Then, under the assumption that the time to evaluate $\pi(\cdot)$ is much larger than the time to evaluate $f(\cdot)$ (trivially true in our SCO environments), this speedup is approximately M . Consequently, the effective speedup provided by Algorithm 1 is $M/\#\text{iterations}$. It is also worth noting that Algorithm 1 allows for the batched application of $\pi(\cdot)$. Specifically, the first application of $\pi(\cdot)$ on each of the M processes can be batched together, following which the second application of $\pi(\cdot)$ on each of these processes can be batched, and so forth.

Our discussion so far applies to general dynamical systems. We cannot hope for an effective speedup in this generality. The next Section will focus on a large class of SCO problems, where we will theoretically establish that Algorithm 1 achieves a non-trivial speedup over sequential computation.

3. Picard Iteration and RL for Supply Chain Optimization

We focus here on the *Fulfillment Optimization* (FO) problem, representative of a class of SCO problems that have been a target for RL algorithms. We are concerned with I products, indexed by $i \in [I]$. Inventory of each product is carried at one or more of J nodes, indexed by $j \in [J]$. Each node is endowed with a processing capacity. Let $c_{t,j} \in \mathbb{R}$ be the remaining capacity of node j at time t . In addition to the capacity constraint, let $x_{t,i,j} \in \mathbb{R}$ be the inventory level of product i at node j and time t . We use $c_t \in \mathbb{R}^J$ and $x_t \in \mathbb{R}^{IJ}$ to simplify the notation. The state at time t is then $s_t := (x_t, c_t)$. An order at time t is associated with a product $i(\omega_t)$ and a reward vector $r(\omega_t) \in \mathbb{R}^J$. A policy π assigns this order to a node with available inventory of product $i(\omega_t)$ and non-zero capacity and earns the corresponding reward (or it does not fulfill and earns zero reward):

$$a_t := \pi(s_t, \omega_t) \in \{j \in [J] \mid c_{t,j} > 0, x_{t,i(\omega_t),j} > 0\} \cup \{0\}$$

where ‘0’ is the action of not fulfilling, i.e., a^ϕ . The goal is to design a policy that maximizes the total reward over some finite horizon T .

The FO problem has state space $\mathcal{S} = \mathbb{R}^{IJ} \times \mathbb{R}^J$ and action space $\mathcal{A} = [J] \cup \{0\}$. Capacity is updated according to $c_{t+1} = c_t - e_{a_t}$ while available inventory is updated according to $x_{t+1} = x_t - e_{i(\omega_t), a_t}$ (where e_j denotes the j th unit vector); this specifies $f(\cdot)$.

There is just one design decision we need to make in considering how to apply the Picard iteration to the FO problem, viz. how to assign time-steps to each of the M processes. We consider the approach of partitioning by products: all time-steps associated with a given product are assigned to the same process. Specifically, let $T_i = \{t : i(\omega_t) = i\}$. Let $[I]$ be divided into M disjoint partitions; denote the m th I_m . Let processor m be responsible for all time-steps associated with products in I_m , i.e., $\mathcal{T}_m = \cup_{i \in I_m} T_i$. Ideally, we find a partition of $[I]$ such that each \mathcal{T}_m is roughly the same size. With this setup, we now state the main result of this section informally:

Theorem 1 (Informal) *Provided $\pi(\cdot)$ satisfies a set of regularity conditions, the Picard iteration, Algorithm 1, converges in at most $J + 1$ iterations for the FO problem.*

Speedup: A corollary of the above result is that Algorithm 1 provides an effective speedup of $T/(J \max_m |\mathcal{T}_m|)$. When tasks are constant sizes, $T/\max_m |\mathcal{T}_m| \sim M$ (see e.g., ‘balls into bins’ problems [34]) so that the speedup provided by Algorithm 1 is $\sim M/J$. As noted in the introduction, even for a large instance of the FO problem (corresponding say to a retailer like Amazon), $J \sim 200$, whereas we can take $M \sim 10^4$ to 10^5 so that we can hope for a speedup on the order of 10^2 to 10^3 .

3.1. Proof of special case

We present here a short proof of Theorem 1 in a special case; the general proof will be presented in the Appendix. For the special case we consider, we assume that (1) inventory is not a constraint (or equivalently that $x_1 = T\mathbf{1}$), and (2) that the policy $\pi(\cdot)$ is greedy (greedy policies have been used widely in practice [12, 13]) so that $\pi(s, \omega) \in \arg \max_{j: c_j > 0} r_j(\omega)$.

The crux of the proof lies in understanding the structural properties of ‘wrong’ actions. To show that a_t^k is correct (i.e., $a_t^k = a_t^{\text{seq}}$), we need to provide that the mistakes made in round $k - 1$ by other processors are constrained in a desired way (they would impact s_t and, therefore, a_t^k). We conducted an inductive proof for showing those properties, where the challenges lie in identifying the ‘right’ induction hypothesis and connecting different structural properties.

For the special greedy case, the ‘right’ structure properties turn out to be related to the set of nodes that run out of capacity in the sequential scenarios. In particular, denote by τ_j the first time at which node j runs out of inventory assuming sequentially correct actions: $\tau_j = \min\{t : c_{t,j}^{\text{seq}} = 0\}$ (or $T + 1$ if $c_{t,j}^{\text{seq}} > 0$ for all $t \in [T]$). Next we define \mathcal{Q}_t to be the set of all nodes that have run out of capacity at some time $t' \leq t$: $\mathcal{Q}_t = \{j \in [J] : \tau_j \leq t\}$. We then have the following invariant:

Lemma 1 *For any $t \in [T]$ and all iterations k of Algorithm 1, we have that the cached action*

$$\alpha_t^k \in \{a_t^{\text{seq}}\} \cup \mathcal{Q}_t.$$

That is to say, the action taken at time t is either going to be correct or will go to a node that would run out of capacity in the sequential scenario. Assuming Lemma 1, we prove Theorem 1 for the special case. Let us denote by $\tilde{\tau}_1, \tilde{\tau}_2, \dots, \tilde{\tau}_J$, the values of τ_j sorted from smallest to greatest. We establish by induction that in iteration k , $\alpha_t^k = a_t^{\text{seq}}$ for all $t < \tilde{\tau}_k$, i.e. the cached action is correct for all times $t < \tilde{\tau}_k$. This establishes a stronger statement: we converge after $|\mathcal{Q}_T| + 1$ iterations.

The induction statement is vacuously true for the initial cache; assume the statement true up to some k , and consider $k + 1$. By the induction hypothesis, at iteration $k + 1$, all processes m have access to the correct cached action for times $t < \tilde{\tau}_k$ so that $a_t^{k+1,m} = a_t^{\text{seq}}$ for $t < \tilde{\tau}_k$. Consequently, $c_t^{k+1,m} = c_t^{\text{seq}}$ for $t \leq \tilde{\tau}_k$, and in particular, $c_{\tilde{\tau}_k,j}^{k+1,m} = 0$ for all $j \in \mathcal{Q}_{\tilde{\tau}_k}$. Now by Lemma 1, we must have that for any $t \in \mathcal{T}_m$ such that $\tilde{\tau}_k \leq t < \tilde{\tau}_{k+1}$,

$$a_t^{k+1,m} \in \{a_t^{\text{seq}}\} \cup \mathcal{Q}_t = \{a_t^{\text{seq}}\} \cup \mathcal{Q}_{\tilde{\tau}_k}.$$

But since $c_{\tilde{\tau}_k,j}^{k+1,m} = 0$ for all $j \in \mathcal{Q}_{\tilde{\tau}_k}$, it must be that $a_t^{k+1,m} = a_t^{\text{seq}}$, so that $\alpha_t^{k+1} = a_t^{\text{seq}}$ for $\tilde{\tau}_k \leq t < \tilde{\tau}_{k+1}$ proving the inductive step and completing the proof. We finish up with proving Lemma 1.

Proof of Lemma 1: Assume the Lemma holds for all $t' \in [T]$ for iterations up to $k - 1$, and for $t' \leq t$ in iteration k . Consider time-step $t + 1$ then and assume that this is handled by processor m . If $a_{t+1}^{k,m} \in \mathcal{Q}_{t+1}$ we are done, and so assume that $a_{t+1}^{k,m} \in [J] \setminus \mathcal{Q}_{t+1}$. Now $a_{t+1}^{\text{seq}} \in \arg \max_{[J] \setminus \mathcal{Q}_{t+1}} r_j(\omega_{t+1})$. So if $c_{t+1,j}^{k,m} > 0$ for all $j \in [J] \setminus \mathcal{Q}_{t+1}$, we are done. Now assume that $a_{t'}^{k,m} = j \in [J] \setminus \mathcal{Q}_{t+1}$ for some $t' \leq t$. By the induction hypothesis, it must be that $j \in \{a_{t'}^{\text{seq}}\} \cup \mathcal{Q}_{t'}$. But $\mathcal{Q}_{t'} \subseteq \mathcal{Q}_{t+1}$, and since $j \in [J] \setminus \mathcal{Q}_{t+1}$ by assumption, it must then be that $j = a_{t'}^{\text{seq}}$. We have consequently shown:

$$c_{t+1,j}^{k,m} = c_{1,j} - \sum_{t' \leq t} \mathbf{1}\{a_{t'}^{k,m} = j\} \geq c_{1,j} - \sum_{t' \leq t} \mathbf{1}\{a_{t'}^{\text{seq}} = j\} = c_{t+1,j}^{\text{seq}} > 0$$

for $j \in [J] \setminus \mathcal{Q}_{t+1}$ completing the proof.

3.2. The general setting

We now remove the restrictions considered in the special case above, allowing for arbitrary initial inventories (so that inventory feasibility matters) and consider a more general class of state-dependent policies. Specifically, we will require that the policy $\pi(\cdot)$ satisfies the following assumptions:

Assumption 1 (Inventory Independence): Fix some $i \in [I]$ and let x and x' be two inventory positions in $\mathbb{R}^{J \times J}$ such that $x_{i,j} = x'_{i,j}$ for all j . Then, if $i(\omega) = i$, we must have $\pi((x, c), \omega) = \pi((x', c), \omega)$. In simple terms, the fulfillment decision for an order of a specific product depends only on the inventory position across all nodes of that product.

Assumption 2 (Consistency): $\pi((x, c), \omega) = j$, and let $i(\omega) = i$. Consider a distinct state (x', c') such that x' differs from x only in its (i, j') th component, and c' differs from c only in its j' component. Then, we must have $\pi((x', c'), \omega) \in \{j, j'\}$.

Assumption 3 (Monotonicity): Let $\pi((x, c), \omega) = j$, and let $i(\omega) = i$. Then, if $x' = x + e_{i,j}$, $\pi((x', c), \omega) = j$, i.e. increasing inventory of product i to the node it was originally fulfilled from by π will not change the fulfillment decision. Similarly, let $c' = c + e_{j'}$ for any j' such that $c_{j'} > 0$. Then, $\pi((x, c'), \omega) = j$. Specifically, adding capacity to any node with positive capacity will not change the fulfillment decision.

Other than monotonicity with respect to node capacity, the requirements above are natural and met by most policies proposed for the FO problem thus far. The condition on monotonicity with respect to node capacity might seem somewhat unnatural at first blush, but is also met by perhaps the most important class of policies proposed for the FO problem, the so-called ‘bid price’ policies [14, 19]³. Having stated these requirements, we can now re-state a refined version of Theorem 1 formally.

Theorem 1 *Provided $\pi(\cdot)$ satisfies Inventory Independence, Consistency and Monotonicity, the Picard iteration, Algorithm 1, converges in at most $Q_T + 1$ iterations for the FO problem.*

The proof of Theorem 1 is more advanced due to the broader class of policies we allow. As the policy can depend on the inventory in a general way, Lemma 1 no longer holds. Instead, we find that the inventory levels maintain certain monotonicity. The formal proof is provided in the appendix. Recall that Q_T represents the number of nodes that reach their capacity limit under the assumption of sequentially correct actions. In scenarios where demand is less than supply, Q_T can be significantly less than J . Consequently, Theorem 1 can be interpreted as an instance-dependent bound for Picard iterations.

4. Experiments with Fulfillment Optimization

This section presents the results of an implementation of the Picard iteration on large scale Fulfillment Optimization (FO) problem instances. We seek to establish a few key points:

Policy Evaluation Speedup: The Picard iteration offers a speedup of **350-450x** over sequential simulation in the FO problem. The speedup scales approximately linearly with batch size and is robust to a variety of problem characteristics.

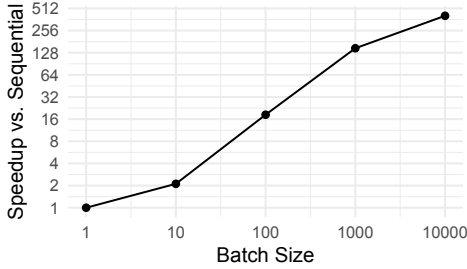
Policy Optimization Speedup: An end-to-end implementation of a policy gradient algorithm on the FO problem highlights the value of our speedup: on a somewhat scaled down instance, time to convergence with sequential evaluation is **~10hrs**; speeding up policy evaluation on that instance with Picard iteration yields the same policy in **2mins**.

Message Passing Degrades Performance: A well regarded scheme for parallel discrete event simulation, Time Warp, allows for no speedup in general policy simulation. Carefully adapting Time Warp to the FO problem yields only a 5x improvement over sequential simulation assuming special structure; on those problems, Picard is **88x** faster than Time Warp.

The source code has been made openly accessible.⁴

³We experimentally demonstrate the robustness of Picard when Assumption 3 violated; see Appendix.

⁴See <https://github.com/aryan-iden-khojandi/policy-simulation-supply-chain-rl>.



β	Product Partitions	Uniform Partitions
0.0	441	363
-0.2	431	360
-0.4	194	361
-0.6	154	358
-0.8	24	354
-1.0	5	355

Figure 1: (left) Picard runtime on problem instances with uniformly distributed demand, as a function of the number of processes i.e., batch size M . y -axis normalizes computation time to that of the $M = 1$ case; i.e. it shows speedup. For $M = 1e4$, we achieve a $441\times$ speedup relative to the sequential algorithm.

Table 1: (right) Speedup of Picard Iteration relative to sequential, as a function of the demand distribution.

4.1. Instance characteristics and practical implementation details

We consider problem instances with $J = 30$ nodes, $I = 1M$ products and $T = 3M$ orders, which is representative of a moderately large-scale real world problem. The distribution of orders per product varies across our experiments (see Section 4.2). The generative model for the reward random variable $r(\omega)$ associated with an order is described in the Appendix. Initial inventory x_1 and capacity c_1 vectors are set roughly so as to be sufficient to manage 80% of orders (so that inventory and capacity constraints are binding); further details are in the Appendix. In all experiments, $\pi(\cdot)$ is implemented as a simple MLP with two layers of width 64.

We implement two practical optimizations that improve performance (but do not impact our theoretical analysis): First, if t_{reset} is the smallest t for which $\alpha_t^k \neq \alpha_t^{k-1}$, then we know that the actions evaluated for times $t < t_{\text{reset}}$ are correct and it is sufficient to start the k th Picard iteration at time $t = t_{\text{reset}}$. Second, as opposed to running Picard iteration over the entire horizon, we run the iteration in ‘chunks’ of size `max_steps` and move on to the next chunk only after convergence of the preceding one. More precisely, we run the **for** loop in Line 5 of the algorithm over $t \in [t_{\text{reset}}, \min(T, t_{\text{reset}} + \text{max_steps})]$. Tuning the `max_steps` parameter thus trades off the need for synchronization (the number of iterations of the **while** loop in Line 2), with the potential for ‘wasting’ computation (the number of iterations of the **for** loop in Line 5).

We consider a high-level (JAX [35]) implementation of Picard that does not require custom kernels. Notably, Line 3 of our algorithm is implemented via `jax.vmap` so that we forego fine-grained control of batching evaluations of $\pi(\cdot)$. All experiments were run on a single A100 GPU with 40GB of VRAM, at 16 bit precision. All key operations are jit-compiled. We also implement the sequential baseline on GPU, where it can leverage parallelism in subroutines such as matrix multiplication.

4.2. Policy evaluation speedup

Here we focus on the speedup afforded by the Picard iteration on policy evaluation. We consider a greedy-like policy approximated by a two-layer, width 64 MLP and consider two sets of experiments:

Uniform Demand, Increasing Batch Size: We divide the T orders across the I products uniformly at random, and vary the batch size M . We determined that our choice of $\pi(\cdot)$ allowed for a batch size of up to $1e4$ and thus vary M in factors of 10 up to $1e4$. Products are assigned to each partition \mathcal{T}_m at random. Recall from our discussion in Section 3, we expect a speedup of $\sim M/J$. Parenthetically, we note that we set `max_steps` here to $300\times M$.

Figure 1 plots our speedup relative to the sequential baseline. We see in all cases a speedup greater than M/J ; in the case of $M = 1e4$ this translates to an actual speedup of **441x**. We observe further that the speedup is largely linear with respect to M , but flags as M grows large. We attribute this to increased conflicts as the number of products assigned to a single partition \mathcal{T}_m decreases.

Heavy-Tailed Demand, Maximum Batch Size: We next consider that the T orders are *not* split uniformly across the I products, but rather that a large fraction of the orders are covered by a disproportionately small fraction of the products. This captures real-world instances accurately. More

precisely, sorting products from those with the most orders associated with them to those with the least, we assume the number of orders for product i , $Q_i \propto i^{-\beta}$. In real-world scenarios typically we expect β in the range of -0.6 to -0.8 [36, 37]; a value of $\beta = 0$ reduces to the uniform demand distribution of the previous paragraph.

We expect this setting to be harder. First, if all orders for a given product were assigned to the same partition \mathcal{T}_m , then we would anticipate significant imbalances in the size of these partitions. In turn this would hurt speedup significantly, since the largest partition would serve to ‘bottleneck’ line 3 of the algorithm (or equivalently, we would limit the opportunities for batching across the partitions \mathcal{T}_m). As an alternative, while this is not covered by our theory, we could simply distribute orders themselves across partitions – i.e. assign each of the T orders uniformly at random to one of the partitions \mathcal{T}_m . This latter setup would serve to make the partitions uniform in size, but intuitively, we would expect a larger number of conflicts (since, for example, multiple partitions now operate on the inventory of a single product). As such, we report results on both approaches to partitioning. Table 1 shows speedup as a function of β for each approach to partitioning. We observe that in fact the latter approach (distributing orders uniformly across partitions) dominates for larger choices of β , i.e. heavy-tailed demand. Irrespective of choice of β , we still see a speedup of at least **350x**.

4.3. End-to-end policy optimization for FO

Finally, we turn to finding an optimal policy for a sequence of FO instances using a policy gradient approach. At each iteration the approach rolls-out the policy at that iterate and computes a policy gradient. We will consider the speedup achieved by computing this roll-out via the Picard iteration, as compared with simply rolling it out sequentially.

In greater detail, we consider the following policy parametrization: let $f_\theta(s) \triangleq [\mu_I^\theta(s), \mu_C^\theta(s)]$ with $\mu_I^\theta(s) \in \mathbb{R}^{IJ}$, $\mu_C^\theta(s) \in \mathbb{R}^J$, be some function of state parameterized by θ ; here we take f_θ to be a two layer MLP of width 64. We then consider the policy

$$\pi_\theta(s_t, \omega_t) \in \arg \max_j (r_j(\omega_t) - \mu_{I,(i(\omega_t),j)}^\theta(s_t) - \mu_{C,j}^\theta(s_t)).$$

Policy gradients for this policy can be computed in analogy to the so-called Dual Mirror Descent Algorithm of [38]. Given the expense of sequential roll-outs here (recall $T = 3M$), we perform just $1e3$ gradient steps. In each step, we perform a gradient update using Adam with learning rate $3e-3$.

Table 2 reports our results for a sequence of problems of increasing size; the largest has $I = 1M$, $T = 3M$ as in our other experiments so far. In each experiment, we report the improvement achieved in policy performance over the starting baseline policy (which was taken to be the greedy policy). We report overall runtime for both sequential policy roll-out and roll-out via the Picard iteration. For the largest problem instance, the sequential implementation takes approximate **10hrs** of wall clock time; whereas using the Picard iteration requires less than **2mins**. We estimate that a further 10x increase in problem size (to 30M orders, 10M products) would require ~ 4 days of computation time with a sequential roll-out, whereas using the Picard iteration for the same would require ~ 5 mins; the sequential figure is estimated based on the time for a single policy gradient iteration.

Problem Scale #Orders/ #Products	Improvement vs Greedy	Runtime Sequential	Runtime Picard
3,000/1,000	19.5%	1m32s	59s
30,000/10,000	20.5%	6m55s	1m01s
300,000/100,000	17.5%	1h04m	1m04s
3,000,000/1,000,000	16.5%	10h02m	1m39s
30,000,000/10,000,000	-	4 days*	4m57s

Table 2: Improvement versus greedy policy and runtimes for different problem scales. Figures with an * are estimated based on a single gradient step.

4.4. A comparison to Time Warp on the GPU

Surprisingly, there is no obvious baseline approach for the parallel policy simulation task. One popular family of approaches to parallel discrete event simulation is the Time Warp algorithm [27, 28, 29, 30] which recently has been adapted to GPUs [31]. The algorithm works roughly as follows: ‘events’

(in the FO case, orders) are assigned to independent processes (just as in our setting). Assuming each process has the correct starting state for some time t_0 , each process executes independently up until some future ‘safe’ time $t_0 + \Delta(t_0)$ taking an arbitrary action (say a^ϕ) on time-steps it was not assigned. Following this, states are synchronized, and $t_0 \leftarrow t_0 + \Delta(t_0)$ or the time of the first ‘conflict’ in $[t_0, t_0 + \Delta(t_0)]$. This is difficult to adapt to general policy simulation: it is unclear that we can define a ‘safe’ $\Delta(t_0)$ and furthermore, a generic approach to detecting conflicts would require sequential simulation (which is what we seek to avoid in the first place).

In attempting to generalize Time Warp, at least to the FO problem, we make the following observation: in the event that a policy for FO satisfies the regularity conditions outlined in Section 3.2 (Assumptions 1, 2 and 3), then choosing $\Delta(t_0) = \min_j c_{t_0,j}$ is a valid choice. Specifically, assuming that all orders for a given product are assigned to the same logical process, we will be guaranteed that $t_0 \leftarrow t_0 + \Delta(t_0)$, i.e. all processes will advance with no roll-backs. We implemented this scheme on the GPU in analogy to [31] for the setting where Picard Iteration achieves its largest speedup: viz. setting $M = 1e4$ and taking uniform demand across all $I = 1\text{M}$ products. Recall from Section 4.2 that Picard achieves a speedup of 441x over sequential simulation in this setup. In contrast we observe that Time Warp achieves a speedup of **5x**. In particular, Picard is **88x** faster than Time Warp, even when the latter is specifically tuned to exploit problem structure.

5. Exploratory Experiments on Environments outside SCO

While we have focused our experiments and analysis on SCO problems, our setup and algorithm apply to *general* environments. This Section briefly explores applying the Picard iteration to environments outside SCO. Specifically, we consider a variety of OpenAI gym MuJoCo environments commonly used for RL benchmarks, implemented in `jax` via the `Brax` library [39]. We consider using the Picard iteration for policy roll-out at each policy optimization iteration in place of sequential simulation. We demonstrate this in the context of PPO [40], although our simulation approach is agnostic to the learning algorithm. Our goal here is simple: we wish to show that Picard iteration converges in a small number of iterations, $\ll T$.

We adopt the network architecture for π , and most policy optimization hyper-parameters from the CleanRL benchmark [41], a popular baseline implementation for RL algorithms. `Jax` training code is adapted from [42], which tries to replicate CleanRL functionality. For numerical stability, we set a learning rate of $3e-5$ and perform one update per trajectory instead of 10.

Setup: For each environment, we run PPO, collecting a total of 100k time-steps. Policy updates occur every 2048 time-steps. We collect the final and penultimate policy iterates which we refer to as π^+ and π^0 respectively. Our goal is to simulate π^+ via Algorithm 1. The additional details that specify this Algorithm to our setting are (1) the choice of M , (2) the assignment of time-steps to partitions \mathcal{T}_m , and (3) the initial choice of cache actions, α_t^0 . We choose to set $M = T = 200$, and as such each \mathcal{T}_m consists of a single time-step.

There is a natural and attractive choice of the initial cache: specifically, we set $\alpha_t^0 = \pi^0(s_t^0, \omega_t)$, the sequence of actions taken by the previous policy iterate on the sample path in question. It is worth pausing to note that this choice of cache is a natural initial draft that is available in general for policy optimization problems; specifically this is the output of Algorithm 1 on π^0 .

Results: Figure 2 plots the convergence of the Picard iteration across several environments, and multiple seeds for each environment. Defining the state trajectory simulated at the k th Picard iteration according to $s_{t-1}^k = f(s_t^k, \alpha_t^k, \omega_t)$, we measure convergence here via relative root-mean-squared-error (RMSE): $\sum_t \|s_t^{+, \text{seq}} - s_t^k\|_2 / \sum_t \|s_t^{+, \text{seq}}\|_2$. This quantity is guaranteed to be 0 (up to numerical precision) for $k = T = 200$ by Proposition 1, but the key question is whether we get convergence in $k \ll T$.

Figure 2 answers this question in the affirmative. We see that in five of eight environments, the relative RMSE (median over 30 random seeds) converges to $\leq 0.1\%$ in **under five iterations whereas** $T = 200$; further, all environments converge within fifteen iterations. These are exciting results that suggest the Picard framework might be of value in general environments as well. For instance if evaluation of f were sufficiently faster than evaluation of π (i.e. if dynamics were cheaper to simulate than policy evaluation), the results here would lead to an end-to-end speedup of **13-40x**.

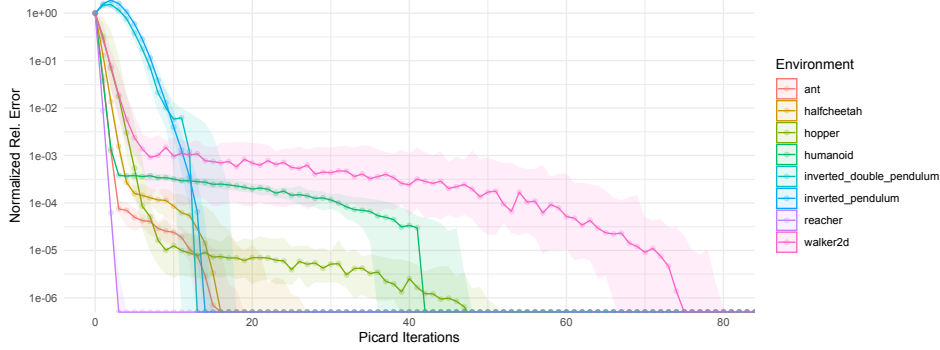


Figure 2: Convergence of the Picard iteration for Gym MuJoCo environments, measured in relative RMSE between the Picard trajectory and the sequentially simulated correct trajectory (normalized by RMSE of the draft trajectory $\{s_t^0\}_{t \in [T]}$). Solid line shows median RMSE at each iteration over 30 seeds; error bars show 20th and 80th percentiles. Median rel. RMSE converges to $\leq 0.1\%$ in under fifteen iterations for all environments, whereas $T = 200$; five of eight converge within 5 iterations.

6. Future Work

There are exciting avenues for future work on the surprisingly under explored problem of speeding up policy simulation:

SCO Problems: Whereas the FO problem is indeed an important class of SCO problems, other classes are problems that involve ‘replenishment’. We believe Picard iteration will provide similar speedups there, and it will be interesting to extend our theoretical development to cover them.

Convergence in Other Environments: We showed promising results for environments outside SCO (viz. MuJoCo), but the success of Picard there is not theoretically understood. It would be interesting to analyze the determinants of convergence in other environments, perhaps beginning with simple time-varying linear systems. Parenthetically, it is simple to show that for a ‘contractive’ system, Picard iteration converges linearly at a rate given by the corresponding contractive factor.

Overall Speedup in Other Environments: Assuming a batch size M and that we require K Picard iterations for convergence, the overall speedup is $(\eta + 1)/(\eta + 1/M)K$. Here η is the ratio of the amount of time it takes to evaluate $f(\cdot)$ to that of evaluating $\pi(\cdot)$. In the case of SCO problems this ratio is ~ 0 . On the other hand, for environments like MuJoCo, this ratio is actually close to $1/5$. As such, we see that speeding up f can result in dramatic time savings in concert with Picard. In the case of MuJoCo for example, this could be achieved with a vectorized physics engine.

References

- [1] Amazon. Supply chain standards, 2024. URL <https://supplychain.amazon.com/>. Accessed: 2024-05-22.
- [2] Walmart. A new era of fulfillment: Introducing walmart’s next generation fulfillment centers, 2022. URL <https://corporate.walmart.com/news/2022/06/03/a-new-era-of-fulfillment-introducing-walmarts-next-generation-fulfillment-centers>. Accessed: 2024-05-22.
- [3] Amazon.com, Inc. Amazon.com, inc. 2023 annual report, 2023.
- [4] Afshin Oroojlooyjadid, MohammadReza Nazari, Lawrence V Snyder, and Martin Takáč. A deep q-network for the beer game: Deep reinforcement learning for inventory optimization. *Manufacturing & Service Operations Management*, 24(1):285–304, 2022.
- [5] Joren Gijsbrechts, Robert N Boute, Jan A Van Mieghem, and Dennis J Zhang. Can deep reinforcement learning improve inventory management? performance on lost sales, dual-sourcing, and multi-echelon problems. *Manufacturing & Service Operations Management*, 24(3):1349–1368, 2022.
- [6] Tarkan Temizöz, Christina Imdahl, Remco Dijkman, Douniel Lamghari-Idrissi, and Willem van Jaarsveld. Deep controlled learning for inventory control. *arXiv preprint arXiv:2011.15122*, 2020.

- [7] Matias Alvo, Daniel Russo, and Yash Kanoria. Neural inventory control in networks via hindsight differentiable policy optimization. *arXiv preprint arXiv:2306.11246*, 2023.
- [8] Dhruv Madeka, Kari Torkkola, Carson Eisenach, Anna Luo, Dean P Foster, and Sham M Kakade. Deep inventory management. *arXiv preprint arXiv:2210.03137*, 2022.
- [9] Jiayi Liu, Shuyi Lin, Linwei Xin, and Yidong Zhang. Ai vs. human buyers: A study of alibaba’s inventory replenishment system. *INFORMS Journal on Applied Analytics*, 53(5):372–387, 2023.
- [10] Meng Qi, Yuanyuan Shi, Yongzhi Qi, Chenxin Ma, Rong Yuan, Di Wu, and Zuo-Jun Shen. A practical end-to-end inventory management model with deep learning. *Management Science*, 69(2):759–773, 2023.
- [11] Jason Acimovic and Vivek F Farias. The fulfillment-optimization problem. In *Operations Research & Management Science in the age of analytics*, pages 218–237. INFORMS, 2019.
- [12] Yanyang Zhao, Xinshang Wang, and Linwei Xin. Multi-item online order fulfillment in a two-layer network. *Chicago Booth Research Paper*, (20-41), 2022.
- [13] Zhen Xu, Hailun Zhang, Jiheng Zhang, and Rachel Q Zhang. Online demand fulfillment under limited flexibility. *Management Science*, 66(10):4667–4685, 2020.
- [14] Kalyan Talluri and Garrett Van Ryzin. An analysis of bid-price controls for network revenue management. *Management science*, 44(11-part-1):1577–1593, 1998.
- [15] Will Ma. Order-optimal correlated rounding for fulfilling multi-item e-commerce orders. *Manufacturing & Service Operations Management*, 25(4):1324–1337, 2023.
- [16] Ayoub Amil, Ali Makhdoumi, and Yehua Wei. Multi-item order fulfillment revisited: Lp formulation and prophet inequality. *Available at SSRN 4176274*, 2022.
- [17] Jason Acimovic and Stephen C Graves. Making better fulfillment decisions on the fly in an online retail environment. *Manufacturing & Service Operations Management*, 17(1):34–51, 2015.
- [18] Stefanus Jasin and Amitabh Sinha. An lp-based correlated rounding scheme for multi-item ecommerce order fulfillment. *Operations Research*, 63(6):1336–1351, 2015.
- [19] John M Andrews, Vivek F Farias, Aryan I Khojandi, and Chad M Yan. Primal–dual algorithms for order fulfillment at urban outfitters, inc. *INFORMS Journal on Applied Analytics*, 49(5): 355–370, 2019.
- [20] Volodymyr Mnih, Adria Puigdomenech Badia, Mehdi Mirza, Alex Graves, Timothy Lillicrap, Tim Harley, David Silver, and Koray Kavukcuoglu. Asynchronous methods for deep reinforcement learning. In *International conference on machine learning*, pages 1928–1937. PMLR, 2016.
- [21] Eric Liang, Richard Liaw, Robert Nishihara, Philipp Moritz, Roy Fox, Ken Goldberg, Joseph Gonzalez, Michael Jordan, and Ion Stoica. Rllib: Abstractions for distributed reinforcement learning. In *International conference on machine learning*, pages 3053–3062. PMLR, 2018.
- [22] Jiayi Weng, Min Lin, Shengyi Huang, Bo Liu, Denys Makoviichuk, Viktor Makoviyichuk, Zichen Liu, et al. Envpool: A highly parallel reinforcement learning environment execution engine. In *Advances in Neural Information Processing Systems*, volume 35, pages 22409–22421, 2022. C++ for environment step parallelization.
- [23] Adam Stooke and Pieter Abbeel. Accelerated methods for deep reinforcement learning. *arXiv preprint arXiv:1803.02811*, 2018. Simple batching for multiple trajectories.
- [24] Alfredo V Clemente, Humberto N Castejón, and Arjun Chandra. Efficient parallel methods for deep reinforcement learning. *arXiv preprint arXiv:1705.04862*, 2017.
- [25] Aleksei Petrenko, Zhehui Huang, Tushar Kumar, Gaurav Sukhatme, and Vladlen Koltun. Sample factory: Ego-centric 3d control from pixels at 100000 fps with asynchronous reinforcement learning. In *International Conference on Machine Learning*, pages 7652–7662. PMLR, 2020.
- [26] Alexander Rutherford, Benjamin Ellis, Matteo Gallici, Jonathan Cook, Andrei Lupu, Gardar Ingvarsson, Timon Willi, Akbir Khan, Christian Schroeder de Witt, Alexandra Souly, et al. Jaxmarl: Multi-agent rl environments in jax. *arXiv preprint arXiv:2311.10090*, 2023.

- [27] Richard M Fujimoto, Rajive Bagrodia, Randal E Bryant, K Mani Chandy, David Jefferson, Jayadev Misra, David Nicol, and Brian Unger. Parallel discrete event simulation: The making of a field. In *2017 Winter Simulation Conference (WSC)*, pages 262–291. IEEE, 2017.
- [28] David Jefferson, Brian Beckman, Frederick Wieland, Leo Blume, and Mike DiLoreto. Time warp operating system. In *Proceedings of the eleventh ACM Symposium on Operating systems principles*, pages 77–93, 1987.
- [29] Jeff S Steinman. Breathing time warp. In *Proceedings of the seventh workshop on Parallel and distributed simulation*, pages 109–118, 1993.
- [30] Peter D Barnes Jr, Christopher D Carothers, David R Jefferson, and Justin M LaPre. Warp speed: executing time warp on 1,966,080 cores. In *Proceedings of the 1st ACM SIGSIM Conference on Principles of Advanced Discrete Simulation*, pages 327–336, 2013.
- [31] Xinhui Liu and Philipp Andelfinger. Time Warp on the GPU: Design and Assessment. In *Proceedings of the 2017 ACM SIGSIM Conference on Principles of Advanced Discrete Simulation*, pages 109–120, Singapore Republic of Singapore, May 2017. ACM. ISBN 978-1-4503-4489-0. doi: 10.1145/3064911.3064912.
- [32] Yichao Fu, Peter Bailis, Ion Stoica, and Hao Zhang. Break the sequential dependency of llm inference using lookahead decoding. *arXiv preprint arXiv:2402.02057*, 2024.
- [33] Xiaosong Li, Wentong Cai, and Stephen John Turner. Gpu accelerated three-stage execution model for event-parallel simulation. In *Proceedings of the 1st ACM SIGSIM Conference on Principles of Advanced Discrete Simulation*, pages 57–66, 2013.
- [34] Martin Raab and Angelika Steger. “balls into bins”—a simple and tight analysis. In *International Workshop on Randomization and Approximation Techniques in Computer Science*, pages 159–170. Springer, 1998.
- [35] James Bradbury, Roy Frostig, Peter Hawkins, Matthew James Johnson, Chris Leary, Dougal Maclaurin, George Necula, Adam Paszke, Jake VanderPlas, Skye Wanderman-Milne, and Qiao Zhang. JAX: composable transformations of Python+NumPy programs, 2018. URL <http://github.com/google/jax>.
- [36] Erik Brynjolfsson, Yu (Jeffrey) Hu, and Michael D. Smith. Consumer Surplus in the Digital Economy: Estimating the Value of Increased Product Variety at Online Booksellers. *Management Science*, 49(11):1580–1596, November 2003. ISSN 0025-1909. doi: 10.1287/mnsc.49.11.1580.20580.
- [37] Erik Brynjolfsson, Yu Jeffrey Hu, and Michael D. Smith. The Longer Tail: The Changing Shape of Amazon’s Sales Distribution Curve, September 2010.
- [38] Haihao Lu, Santiago Balseiro, and Vahab Mirrokni. Dual mirror descent for online allocation problems. *arXiv preprint arXiv:2002.10421*, 2020.
- [39] C. Daniel Freeman, Erik Frey, Anton Raichuk, Sertan Girgin, Igor Mordatch, and Olivier Bachem. Brax - a differentiable physics engine for large scale rigid body simulation, 2021. URL <http://github.com/google/brax>.
- [40] John Schulman, Filip Wolski, Prafulla Dhariwal, Alec Radford, and Oleg Klimov. Proximal policy optimization algorithms. *arXiv preprint arXiv:1707.06347*, 2017.
- [41] Shengyi Huang, Rousslan Fernand Julien Dossa, Chang Ye, Jeff Braga, Dipam Chakraborty, Kinal Mehta, and João G.M. Araújo. Cleanrl: High-quality single-file implementations of deep reinforcement learning algorithms. *Journal of Machine Learning Research*, 23(274):1–18, 2022. URL <http://jmlr.org/papers/v23/21-1342.html>.
- [42] Chris Lu, Jakub Kuba, Alistair Letcher, Luke Metz, Christian Schroeder de Witt, and Jakob Foerster. Discovered policy optimisation. *Advances in Neural Information Processing Systems*, 35:16455–16468, 2022.

A. Appendix / supplemental material

A.1. Proof of Proposition 1

We will prove the proposition by induction on the following hypothesis: $\alpha_t^k = a_t^{\text{seq}} \quad \forall t \leq k$, hence the desired result will follow immediately by setting $k = T$. Letting \tilde{m}_t^k denote the processor to which order t is assigned in iteration k , we have $\alpha_1^1 = a_1^{1, \tilde{m}_1^1} = a_1^{\text{seq}}$, since all processors have the correct state at the beginning of the horizon: $s_1^{1, m} = s_1 \quad \forall m$. Now, assume that $\alpha_t^k = a_t^{\text{seq}} \quad \forall t \leq k$. By this induction hypothesis (and the state update defined in Section 3), we have $s_k^{k, m} = s_k \quad \forall m$. Therefore, processor \tilde{m}_{k+1}^{k+1} makes the right decision for order $k+1$, and we have: $\alpha_{k+1}^{k+1} = a_{k+1}^{k+1, \tilde{m}_{k+1}^{k+1}} = a_{k+1}^{\text{seq}}$. ■

A.2. Proof of Theorem 1

We will use the following lemma, which will facilitate greatly the proof of Theorem 1.

Lemma 2 *Let $Q_t := \{j \in [J] \mid \tau_j \leq t\}$ be the set of nodes that run out of capacity before t in the sequential scenario. We have, at any iteration $k \geq 1$, any time step $t \in [T]$, any product $i \in [I]$ and any process $m \in [M]$*

$$x_{t, i, j}^{k, m} \geq x_{t, i, j}^{\text{seq}}, \forall j \notin Q_t \quad (1)$$

$$c_{t, j}^{k, m} \geq c_{t, j}^{\text{seq}}, \forall j \notin Q_t. \quad (2)$$

Proof of Theorem 1. We will invoke Lemma 2 for the proof. To begin, we state that for all $k \geq 1$, the following holds

$$\alpha_t^k = a_t^{\text{seq}}, 1 \leq t \leq \tilde{\tau}_k. \quad (3)$$

We can see that (3) directly implies Theorem 1. We proceed to prove (3) by induction, assuming it holds when $1 \leq k < k_c$. We want to prove the case for $k = k_c$. By induction, we have $x_{\tilde{\tau}_{k_c-1}, i, j}^{k_c, m} = x_{\tilde{\tau}_{k_c-1}, i, j}^{\text{seq}}$ and $c_{\tilde{\tau}_{k_c-1}, j}^{k_c, m} = c_{\tilde{\tau}_{k_c-1}, j}^{\text{seq}}$ for all $i \in [I], j \in [J]$ and $m \in [M]$. In particular, the set of nodes $\{j \in [J], c_{\tilde{\tau}_{k_c-1}, j}^{k_c, m} = 0\} = \{j \in [J], c_{\tilde{\tau}_{k_c-1}, j}^{\text{seq}} = 0\} = Q_{\tilde{\tau}_{k_c}}$ have run out of capacity at time $\tilde{\tau}_{k_c-1}$ for both the local process m and the sequential scenario.

Now, consider $t \in [\tilde{\tau}_{k_c-1} + 1, \tilde{\tau}_{k_c})$, we have that in the sequential scenario no node is running out of capacity during this period (note that the next depleted one is at $\tilde{\tau}_{k_c}$). Therefore $Q_t = Q_{\tilde{\tau}_{k_c}}$ and $c_{t, j}^{\text{seq}} > 0 \forall j \notin Q_{\tilde{\tau}_{k_c}}$. Then by Lemma 2, we have that for $t \in [\tilde{\tau}_{k_c-1} + 1, \tilde{\tau}_{k_c})$,

$$c_{t, j}^{k_c, m} \geq c_{t, j}^{\text{seq}} > 0, \forall j \notin Q_{\tilde{\tau}_{k_c}}.$$

Therefore, for $t \in [\tilde{\tau}_{k_c-1} + 1, \tilde{\tau}_{k_c})$, the process m maintains the same feasible set of fulfillment nodes as the sequential scenario:

$$\{\mathbf{1}(c_{t, j}^{k_c, m} > 0)\}_{j \in [J]} = \{\mathbf{1}(c_{t, j}^{\text{seq}} > 0)\}_{j \in [J]}.$$

Now consider an arbitrary product $i_c \in [I]$ and its orders \mathcal{A} within the time period $[\tilde{\tau}_{k_c-1} + 1, \tilde{\tau}_{k_c}]$: $\mathcal{A} \subset [\tilde{\tau}_{k_c-1} + 1, \tilde{\tau}_{k_c}]$. The orders in \mathcal{A} is processed sequentially by a process and for any $t \in \mathcal{A}$, we aim to show

$$\begin{aligned} a_t^{k_c} &= a_t^{k_c, m} = \pi(\{x_{t-1, i_c, j}^{k_c, m}\}_{j \in [J]}, \{\mathbf{1}(c_{t-1, j}^{k_c, m} > 0)\}_{j \in [J]}, \omega_t) \\ &= \pi(\{x_{t-1, i_c, j}^{\text{seq}}\}_{j \in [J]}, \{\mathbf{1}(c_{t-1, j}^{\text{seq}} > 0)\}_{j \in [J]}, \omega_t) \\ &= a_t^{\text{seq}}. \end{aligned}$$

This is evident since the capacity-feasible set remains identical between the local process and the sequential process, and the inventory levels $x_{t, i_c, j}^{k_c, m}$ and $x_{t, i_c, j}^{\text{seq}}$ share the same initial points at time $\tilde{\tau}_{k_c-1}$ and are solely determined by the fulfillment decisions made for product i_c at $t \in \mathcal{A}$. Thus all states and decisions remain the same between the local process and the sequential process during $[\tilde{\tau}_{k_c-1} + 1, \tilde{\tau}_{k_c}]$. This completes the proof. ■

A.2.1. Proof of Lemma 2

Note that the capacity consumed at a node is the sum of the inventories consumed at that node. Therefore, for given $j \in [J], t \in [T], x_{t,i,j}^{k,m} \geq x_{t,i,j}^{\text{seq}}$ for all $i \in [I]$ implies that $c_{t,j}^{k,m} \geq c_{t,j}^{\text{seq}}$. Thus it is sufficient to show (1).

We prove this by induction. (1) holds for $k = 0$ since all orders are not fulfilled and all inventories are not consumed. For any given $k_c \in \mathbb{N}, t_c \in [T]$, assume this holds for any $0 \leq k < k_c, t \in [T]$ and $k = k_c, 1 \leq t < t_c$. Now we want to prove (1) for $k = k_c, t = t_c$.

Consider a process m associated with product subset \mathcal{A}_m and order subset \mathcal{P}_m . Let the product at time t_c be i_c . It is sufficient to show

$$x_{t_c, i_c, j}^{k,m} \geq x_{t_c, i_c, j}^{\text{seq}}, \forall j \notin Q_{t_c} \quad (4)$$

since the inventory levels for other products will remain the same in processing order t_c .

If i_c is handled by a process m' that is not m , i.e., $i_c \in \mathcal{A}_{m'} \neq \mathcal{A}_m$, m will skip the invocation of π and take $a_{t_c}^{k,m} = a_{t_c}^{k-1, m'}$. In fact, this skip will occur for every order related to i_c , i.e., $a_t^{k,m} = a_t^{k-1, m'}$ for all $t \in [T]$ with $i(\omega_t) = i_c$. This implies that the inventory level for i_c at process m is the same as the inventory level at m' from the previous iteration, thus (4) holds by induction:

$$x_{t_c, i_c, j}^{k,m} = x_{t_c, i_c, j}^{k-1, m'} \geq x_{t_c, i_c, j}^{\text{seq}}, \forall j \notin Q_{t_c}.$$

Next we consider the case i_c is handled by process m , i.e., $i_c \in \mathcal{A}_m$. Recall that the dynamics of the states are

$$\begin{aligned} x_{t_c, i_c, j}^{k,m} &= x_{t_c-1, i_c, j}^{k,m} - \mathbf{1}(a_{t_c}^{k,m} = j) \\ c_{t_c, j}^{k,m} &= c_{t_c-1, j}^{k,m} - \mathbf{1}(a_{t_c}^{k,m} = j). \end{aligned}$$

We aim to show that even the decision $a_{t_c}^{k,m}$ is wrong, meaning not the same as $a_{t_c}^{\text{seq}}$, the inventory monotonicity in (4) still hold. Specifically, we will show

$$a_{t_c}^{k,m} \in \{a_{t_c}^{\text{seq}}\} \cup Q_{t_c} \cup \{j \notin Q_{t_c}, x_{t_c-1, i_c, j}^{k,m} > x_{t_c-1, i_c, j}^{\text{seq}}\}. \quad (5)$$

(5) implies that when $a_{t_c}^{k,m} \neq a_{t_c}^{\text{seq}}$, we have either $a_{t_c}^{k,m} \in Q_{t_c}$, which is excluded when examining (4), or $a_{t_c}^{k,m} \in \{j \notin Q_{t_c}, x_{t_c-1, i_c, j}^{k,m} > x_{t_c-1, i_c, j}^{\text{seq}}\}$, which will maintain the inventory monotonicity after the state update. Thus, (5) implies (4).

To prove that (5) holds, we examine the capacity level at time t_c . Note that the capacity consumed is the aggregation of inventories consumed at any time point, thus for all $j \notin Q_{t_c}$,

$$\begin{aligned} c_{t_c-1, j}^{k,m} &= c_{0, j} - \sum_{i \in [I]} (x_{0, i, j} - x_{t_c-1, i, j}^{k,m}) \\ &\geq c_{0, j} - \sum_{i \in [I]} (x_{0, i, j} - x_{t_c-1, i, j}^{\text{seq}}) && \text{by induction} \\ &= c_{t_c-1, j}^{\text{seq}}. \end{aligned}$$

Thus, both capacity and inventory for the node $j \notin Q_{t_c}$ satisfy the monotonicity comparing to the sequential scenario:

$$c_{t_c-1, j}^{k,m} \geq c_{t_c-1, j}^{\text{seq}} \quad (6)$$

$$x_{t_c-1, i, j}^{k,m} \geq x_{t_c-1, i, j}^{\text{seq}}. \quad (7)$$

We are going to use (6), (7), Assumptions 1-3 to show (5). Note that following our requirements for π given by Assumption 3

$$\pi(\{x_{t_c-1, i_c, j}^{\text{seq}}\}_{j \in [J]}, \{\mathbf{1}(c_{t_c-1, j}^{\text{seq}} > 0)\}_{j \in [J]}, \omega_{t_c}) = a_{t_c}^{\text{seq}}. \quad (8)$$

By Assumption 2, we can replace the inventory and capacity of the nodes in the set Q_{t_c} by $x_{t_c-1,i_c,j}^{k,m}, c_{t_c-1,j}^{k,m}$ and obtain

$$\begin{aligned} & \pi \left(\{x_{t_c-1,i_c,j}^{\text{seq}}\}_{j \notin Q_{t_c}} \cup \{x_{t_c-1,i_c,j}^{k,m}\}_{j \in Q_{t_c}}, \{\mathbf{1}(c_{t_c-1,j}^{\text{seq}} > 0)\}_{j \notin Q_{t_c}} \cup \{\mathbf{1}(c_{t_c-1,j}^{k,m} > 0)\}_{j \in Q_{t_c}}, \omega_{t_c} \right) \\ & \in \{a_{t_c}^{\text{seq}}\} \cup Q_{t_c}. \end{aligned} \quad (9)$$

Note that $c_{t_c-1,j}^{\text{seq}} > 0$ for $j \notin Q_{t_c}$ by the definition of Q_{t_c} (the set of nodes running out of capacity before t_c , i.e., $Q_{t_c} = \{j | c_{t_c-1,j}^{\text{seq}} = 0\}$). Together this with (6), we have $\mathbf{1}(c_{t_c-1,j}^{\text{seq}} > 0) = \mathbf{1}(c_{t_c-1,j}^{k,m} > 0)$ for $j \notin Q_{t_c}$. Thus (10) can be simplified to

$$\pi(\{x_{t_c-1,i_c,j}^{\text{seq}}\}_{j \notin Q_{t_c}} \cup \{x_{t_c-1,i_c,j}^{k,m}\}_{j \in Q_{t_c}}, \{\mathbf{1}(c_{t_c-1,j}^{k,m} > 0)\}_{j \in [J]}, \omega_{t_c}) \in \{a_{t_c}^{\text{seq}}\} \cup Q_{t_c}. \quad (10)$$

Finally, by invoking Assumption 2-3 on the set of $\{j \notin Q_{t_c}, x_{t_c-1,i_c,j}^{k,m} > x_{t_c-1,i_c,j}^{\text{seq}}\}$ and replace $x_{t_c-1,i_c,j}^{\text{seq}}$ by $x_{t_c-1,i_c,j}^{k,m}$, one can verify that

$$\begin{aligned} a_{t_c}^{k,m} & := \pi(\{x_{t_c-1,i_c,j}^{k,m}\}_{j \in [J]}, \{\mathbf{1}(c_{t_c-1,j}^{k,m} > 0)\}_{j \in [J]}, \omega_{t_c}) \\ & \in \{a_{t_c}^{\text{seq}}\} \cup Q_{t_c} \cup \{j \notin Q_{t_c}, x_{t_c-1,i_c,j}^{k,m} > x_{t_c-1,i_c,j}^{\text{seq}}\}. \end{aligned}$$

Thus (5) holds and this completes the proof. \blacksquare

A.3. Details of Problem Setup and Data-Generation Process

As stated briefly in Section 4.1, our experiments use synthetic data based broadly on fulfillment-network and demand-distribution patterns observed at modern (moderately) large industrial-scale retailers. We consider a fulfillment network comprising $J = 30$ nodes located in the 30 most-populous states (each one in the most-populous city of the corresponding state). Although the distribution of demand among products was varied in certain experiments, in all cases, we provided sufficient inventory and fulfillment capacity at the network level (i.e. across all J nodes) to permit the fulfillment of 80% of demand (not accounting for occasional cases of ‘stranded’ inventory, in which one is unable to use inventory left over at a node with no remaining capacity). For each product, i , the network inventory was distributed across nodes *pro rata* based on population: $x_{0,i,j} \propto \text{population}_j$; similarly, network capacity was distributed *pro rata* across nodes based on population: $c_{0,j} \propto \text{population}_j$. For each (order, node) pair (t, j) , we computed the distance between the zip codes, d_{tj} , and then defined a reward for fulfilling Order t from Node j as follows:

$$r_j(\omega_t) = \frac{\max_j d_{tj} - d_{tj}}{\max_j d_{tj}}. \quad (11)$$

Finally, a^ϕ (the always-feasible action) was associated with a zero reward and had ties broken against it to ensure that we only choose it in the absence of any feasible alternatives.

A.4. Practical performance with capacity-dependent policies

The bound on number of iterations until convergence in Section 3.2 assumes that the fulfillment policy does not depend on node capacity. As a final robustness check, however, we are interested in gauging the empirical performance of Picard Iteration for policies that *do* depend on capacity (beyond ensuring feasibility), a regime for which our theory does not directly apply. We therefore conduct an ablation study using a simplified version of the policy that penalizes capacity usage at low-capacity nodes using shadow prices, with strength modulated by a parameter γ . Ranging γ from 0 to ∞ interpolates between a closest-node policy and a policy that always fulfills from the node with greatest remaining capacity (an unrealistic extreme scenario); for reference, a value of $\gamma = 1.0$ allows the node with greatest remaining capacity to improve its ranking by up to $J - 1$ positions (i.e. even the most-expensive node may be chosen if its remaining capacity is sufficiently attractive). The results are shown in Table 3 and demonstrate that empirically, the constraint on capacity (non-)dependence is non-vacuous but can be relaxed substantially: Performance is virtually unchanged for realistic settings of γ that incorporate shadow costs on capacity.

Table 3: Ablation study on a policy that discounts node proximity by (remaining) capacity scarcity

γ	Conflicts	Speedup
0 (no capacity dependence)	13	441x
0.5	14	427x
1.0	15	401x